

# Frequency dependence of $Q$ in Earth's upper mantle inferred from continuous spectra of body waves

Azusa Shito, Shun-ichiro Karato, and Jeffrey Park

Department of Geology and Geophysics, Yale University, New Haven, Connecticut, USA

Received 26 January 2004; revised 13 April 2004; accepted 17 May 2004; published 18 June 2004.

[1] The frequency dependence of  $Q$  in Earth's upper mantle is investigated using the continuous  $P$  wave spectra over  $0.08 < f < 8.0$  Hz. Regional waveform data from 23 events in the Pacific slab recorded on broadband stations in western Japan were used to create spectral ratio estimates of  $P$  waves which sample a subducting slab and mantle wedge. We assumed the power-law model  $Q(f) = Q_0(f/f_0)^\alpha$  and applied a grid search to determine the best fit  $\alpha$  and  $Q_0$ . The inferred frequency dependence ( $0.2 < \alpha < 0.4$ ) in most regions is consistent with laboratory data on solid olivine but not on partially molten olivine-rich rocks except those data for deep events. Close agreement between seismological and laboratory observations on frequency dependence of  $Q$  suggests that physical mechanisms of seismic wave attenuation are common and therefore laboratory data can be used to infer the physical state of Earth's upper mantle from seismic wave attenuation. **INDEX TERMS:** 5144 Physical Properties of Rocks: Wave attenuation; 7218 Seismology: Lithosphere and upper mantle; 8162 Tectonophysics: Rheology—mantle. **Citation:** Shito, A., S. Karato, and J. Park (2004), Frequency dependence of  $Q$  in Earth's upper mantle inferred from continuous spectra of body waves, *Geophys. Res. Lett.*, *31*, L12603, doi:10.1029/2004GL019582.

## 1. Introduction

[2] The frequency dependence of seismic wave attenuation is often ignored in seismological studies of attenuation (for review see *Romanowicz and Durek* [2000]), but it is important for several reasons. First, most laboratory attenuation studies show power-law dependence  $Q \propto f^\alpha$  ( $f$ : frequency) with  $\alpha = 0.2$ – $0.4$  for most solid materials [e.g., *Jackson*, 2000]. If indeed  $Q$  depends on frequency, then  $Q$  estimation from a broad range of frequency should incorporate the frequency dependence of  $Q$ . Second, the frequency dependence of  $Q$  in partially molten peridotites appears to be different from that in solid olivine [*Jackson et al.*, 2004; *Faul et al.*, 2004]. Therefore the presence of partial melt could be detected through the frequency dependence of  $Q$ . Third, recent studies suggest a close connection between  $Q$  and long term rheology [e.g., *Karato and Spetzler*, 1990; *Jackson*, 2000] but the exact relation depends on the frequency dependence of  $Q$  ( $Q \propto \eta^\beta$ ,  $\beta \propto \alpha$ ). Therefore one needs to know the frequency dependence of  $Q$  to convert seismic measurements to the long term viscosity.

[3] Most previous studies of frequency dependent seismic wave attenuation rely on differences in attenuation estimated from several discrete frequency bands [e.g., *Sipkin and Jordan*, 1979; *Flanagan and Wiens*, 1998]. However, because widely separated frequency bands were used, the frequency dependence of attenuation within the gaps is unconstrained. To verify a power-law model for  $Q$ , we need spectrum estimates over a continuous frequency band.

[4] Two previous studies on frequency dependent  $Q$  have used continuous spectrum estimates. *Ulug and Berckhemer* [1984] used a  $S$ – $P$  spectral ratio method in the frequency range 0.03–1.5 Hz. They proposed an absorption band model with a power-law  $Q \propto f^\alpha$  with an exponent  $0.25 < \alpha < 0.6$  in the frequency range up to 1 Hz. *Cheng and Kennett* [2002] also used the  $S$ – $P$  spectral ratios to obtain a power-law with an exponent of  $0.2 < \alpha < 1.0$  in the frequency range up to 6.0 Hz. Their results suggest significant spatial variation of the frequency dependence. For both these studies, the upper range of possible  $\alpha$  is inconsistent with laboratory experimental results [e.g., *Berckhemer et al.*, 1982; *Jackson et al.*, 2002] in the frequency range  $10^{-4}$ –30 Hz. Also, there is no evidence from the laboratory studies for a change of the frequency dependence within the measured frequency range. The  $S$ – $P$  spectral ratio used in the previous two studies is potentially powerful, however in the data set we report in this paper, the  $S$ – $P$  spectral ratio can be biased at higher frequency (>2.5–3.0 Hz) due to the persistence of  $P$  coda energy in the  $S$  wave arrival window. Although the bias threshold (2.5–3.0 Hz in our case) should change from site to site, large values of  $\alpha$  ( $\alpha > 0.6$ ) in *Ulug and Berckhemer* [1984] and *Cheng and Kennett* [2002] might come from the contamination of the  $P$  coda energy.

[5] The aim of this study is to determine the frequency dependence of  $Q$  using a more reliable continuous spectrum estimate over a broader frequency band to better understand the physical mechanism of  $Q$  in Earth's upper mantle.

## 2. Theory of Spectral Ratio Method

[6] The  $P$ – $P$  spectral ratio method [*Roth et al.*, 1999] compares the relative high frequency decay of two  $P$  waves from the same earthquake which travel through slab and mantle above it. The ratio of two phases cancels the most effects of the source time function. Here, less attenuated  $P$  waves which sample mainly in a high- $Q$  slab serve as a reference (Figure 1a). We call the  $P$  waves which sample mainly in mantle and slab as  $P_M$  and  $P_S$  waves, respectively. We also use the words “mantle station” and “slab station” to express the stations which record  $P_M$  and  $P_S$  waves, respectively.

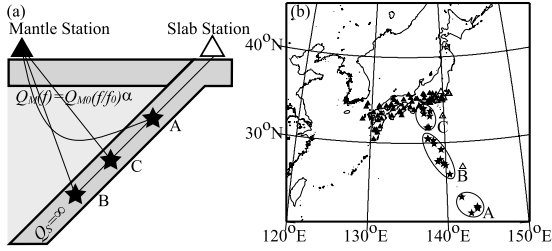


**Figure 1.** (a) Geometry of representative  $P$  wave raypaths from events in three event-groups. Events are shown in stars. Black and white triangles indicate “mantle stations” and “slab stations”, respectively. (b) Events and stations used in this study.

[7] The amplitude spectra of recorded  $P$  waves can be expressed by

$$A_M(f) = C_M \cdot I(f) S_M(f) R_M(f) \exp \left[ -\pi f \int \frac{dT_M}{Q_M(f)} \right] \quad (1)$$

$$A_S(f) = C_S \cdot I(f) S_S(f) R_S(f) \exp \left[ -\pi f \int \frac{dT_S}{Q_S(f)} \right] \quad (2)$$

where  $f$  is frequency,  $C$  is a constant containing the radiation pattern and geometrical spreading effects.  $I(f)$  is the instrument response,  $S(f)$  is the source spectrum,  $R(f)$  is the site response, and the last factor is the attenuation function.  $Q$  is seismic quality factor which depends on frequency and  $dT$  is the differential travel time. The subscripts  $M$  and  $S$  indicate mantle and slab, respectively.

[8] The instrument response  $I(f)$  is known and corrected. The source spectra  $S_M(f)$  and  $S_S(f)$  can be assumed to be same, because we did not use large ( $m_b > 7$ ) events which may exhibit directivity effects. Furthermore, source mechanisms in our data set show randomly oriented rupture directions, which should dampen any directivity effect in a large data set. The ratio of the two Fourier amplitude spectra can be expressed as a natural logarithm

$$\ln \left[ \frac{A_M(f)}{A_S(f)} \right] = c + \ln \left[ \frac{R_M(f)}{R_S(f)} \right] + \left( -\pi f \int \frac{dT_M}{Q_M(f)} + \pi f \int \frac{dT_S}{Q_S(f)} \right) \quad (3)$$

with  $c \equiv \ln [C_M/C_S]$ . Assuming that the attenuation in the slab is extremely small,  $Q_S(f) \sim \infty$  [Shito and Shibutani, 2003], we can neglect the attenuation function of the  $P_S$  wave.

$$\ln \left[ \frac{A_M(f)}{A_S(f)} \right] = c + \ln \left[ \frac{R_M(f)}{R_S(f)} \right] - \pi f \int \frac{dT_M}{Q_M(f)} \quad (4)$$

We assume that  $Q_M^{-1}$  has the power-law frequency dependence,  $Q_M^{-1}(f) = Q_{M0}^{-1} \cdot (ff_0)^{-\alpha}$  where,  $Q_{M0}^{-1}$  is the  $Q_M^{-1}$  at  $f_0$  (1 Hz). We define differential attenuation operator at  $f_0$  (1 Hz) as follows,

$$\delta t_0^* \equiv \int \frac{dT_M}{Q_{M0}} \quad (5)$$

The spectral ratio of the  $P_M$  and  $P_S$  waves can be expressed as

$$\ln \left[ \frac{A_M(f)}{A_S(f)} \right] = c + \ln \left[ \frac{R_M(f)}{R_S(f)} \right] - \pi f \cdot \delta t_0^* \cdot \left( \frac{f}{f_0} \right)^{-\alpha} \quad (6)$$

The spectral ratio curve of  $P_M$  to  $P_S$  can be expressed by equation (6) which is a sum of attenuation function and site response. For  $\alpha > 0$  attenuation is weaker at higher frequencies, relative to a medium with constant  $Q$ . Using  $\alpha = 0.3$  as an example, the value of  $Q$  at 5 Hz would be 62% higher than  $Q$  at 1 Hz.

### 3. Data and Analysis

[9] High quality  $P$  waveform data were provided from two broadband seismograph networks in Japan, F-net (formerly FREESIA) and J-array. We used regional waveform data from 23 events in the vicinity of the Pacific slab which were recorded at 58 stations in western Japan from 1998 to 2002. The origin times and the locations were taken from catalogues of IRIS and JMA. The events ranged in depth from 87 to 520 km with body wave magnitudes  $4.3 \leq m_b \leq 6.8$ .

[10] Events are classified into three groups. Event-group A includes events from 100–200 km depth and the epicentral distance of 11–15°, event-group B from 400–500 km depth and the epicentral distance of 6–10°, event-group C from 300–400 km depth and the epicentral distance of 1–5° (Figure 1).

[11] Figure 2 illustrates the process to make the spectral ratio curve. The  $P_M$  and  $P_S$  waves were taken from the vertical component (Figures 2a and 2b). The length of the time window is 5 s before and 15 s after the onset of  $P$  waves. A fast Fourier transform computed the amplitude spectra after the data were 10% cosine tapered and normalized to the maximum amplitude. The spectra were

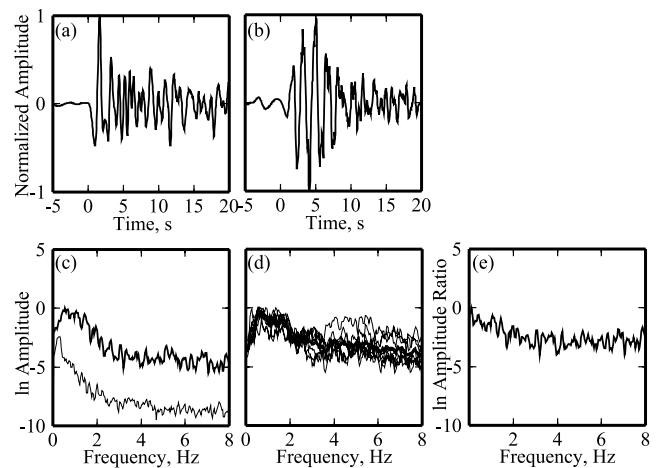


**Figure 2.** (a) A typical waveform of  $P_M$  wave. (b) A typical waveform of  $P_S$  wave. (c) Natural logarithm of amplitude spectra of  $P_M$  wave. Noise spectra are also indicated by thin line. (d) Natural logarithm of amplitude spectra of  $P_S$  wave. Individual and averaged spectra are expressed by thin and thick lines, respectively. (e) Spectral ratio of  $P_M$  to  $P_S$  waves.

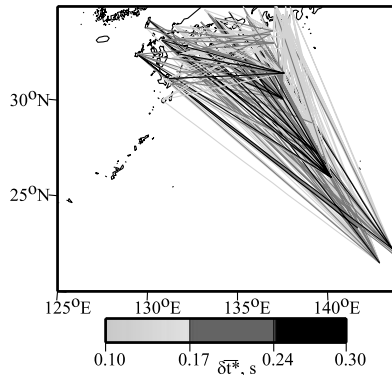


**Figure 3.** The raypaths of  $P_M$  wave used in this study. The  $\overline{\delta t^*}$  is indicated by the tone.

smoothed using a Hanning window with the bandwidth of 0.1 Hz. Figure 2c shows the natural log amplitude spectrum of a  $P_M$  wave. A sample of the noise spectra (thin line) which is taken from 25 to 5 s before the  $P_M$  wave arrival are also shown to evaluate the data quality. High signal to noise ratio can be seen. The frequency band used was 0.08–8.0 Hz, which was determined taking into account the signal to noise ratio. Figure 2d shows the natural log amplitude spectrum of a  $P_S$  wave. To avoid a specific site effect, the reference slab spectrum is made from average (thick line) of individual spectrum (thin line) of more than three  $P_S$  waves. The spectral division of the  $P_M$  wave and the reference  $P_S$  wave was carried out for each frequency point (frequency sampling is 0.04 Hz). The spectral ratios are shown in Figure 2e. We obtained a total of 338 spectral ratio curves for the raypaths shown in Figure 3.

[12] We here argue that attenuation integrated along the raypath dominates the frequency dependence of equation (6). The constant  $c$  is typically small (see Figure 2e). The site effect factor  $R_M(f)/R_S(f)$  must be considered in detail. Our model equation (6) for frequency dependent  $Q$  implies less attenuation at high frequencies, relative to constant  $Q$ . Site effects could replicate this effect in our spectral ratios if near receiver structure amplifies high frequency seismic amplitude at a “mantle station”, or else decreases the high frequency amplitude at a “slab station”. It seems unlikely, however, that such site effects would be consistent among all “mantle station” and “slab station” in Japan. We would expect considerable variation in  $R_M(f)/R_S(f)$  from site to site. Figure 3 shows  $\overline{\delta t^*}$  for each raypath. The  $\overline{\delta t^*}$  is the attenuation averaged over the frequency range which can be defined by the slope of the linear regression line of the spectral ratio curve. The  $\overline{\delta t^*}$  for similar raypaths show similar values. There is only small scatter in the spectral ratio curves obtained from stations with similar raypaths, which argues against the strong influence of near site structure. As a working assumption, we take  $R_M(f)/R_S(f)$  to be constant with frequency and small. Neglecting the constant terms, the differential attenuation operator reduces to the effect of the mantle attenuation function

$$\ln \left[ \frac{A_M(f)}{A_S(f)} \right] = -\pi f \cdot \delta t_0^* \cdot \left( \frac{f}{f_0} \right)^{-\alpha} \quad (7)$$

The spectral ratio of  $P_M$  to  $P_S$  is expressed by a power-law in equation (7), where the exponent  $\alpha$  and constant factor

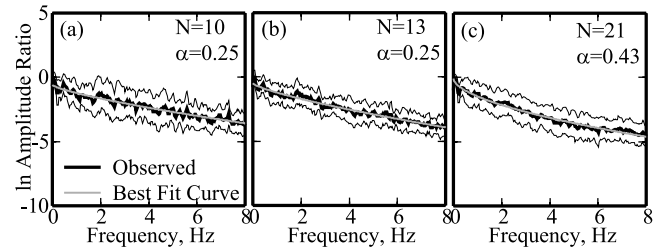


**Figure 4.** Examples for fitting of stacked spectral ratio curves in event-group A. Stacks are made from individual spectral ratio curve whose  $\overline{\delta t^*}$  is 0.10–0.12 for (a), 0.12–0.14 for (b), 0.14–0.16 for (c). The numbers of stacked individual spectra ratio curves ( $N$ ) are indicated at the top right. Observed and the best fit spectral ratio curves are expressed by black and grey lines. Thin lines show range of standard deviation of the stacked spectral ratio curve.

$\delta t_0^*$  reflect the frequency dependence and a reference value of  $Q$ , respectively.

#### 4. Optimum Model of Frequency Dependence of $Q$

[13] We applied a grid search method to determine the best fit values of frequency dependence  $\alpha$  and the reference attenuation  $\delta t_0^*$  in the parameterized model Equation (7) for observed spectral ratios. Fitting the individual spectral ratio estimates is relatively difficult due to random fluctuation of the spectra. To reduce scatter, we stacked the logarithms of spectral ratio estimates from neighboring raypaths and similar  $\overline{\delta t^*}$ . We computed stacked spectral ratio estimates from the 338 individual data, with 6 for event-group A, 8 for event-group B, and 3 for event-group C. Each stack is made from 8–30 pairwise spectral ratio estimates.

[14] For each stack, we estimated the optimum  $\alpha$  and  $\delta t_0^*$ . The grid spacing for the  $\alpha$  is  $\Delta\alpha = 0.01$  from 0.00 to 1.00 and for  $\Delta\delta t_0^* = 0.01$  s from 0.01 to 1.00 s. This range is enough to cover the possible values which are expected concerning the average attenuation of  $P$  wave in this region ( $Q \sim 200$ , from Shito and Shibutani [2003]) and observed travel times  $50 < T < 250$  s. All stacks can be fit well by the power-law model (Figure 4). The frequency dependence of  $Q$  with positive values of  $\alpha$  results in concave-upward curvature in the spectral ratio curves (Figure 4). If  $Q$  is frequency independent (i.e.,  $\alpha = 0$ ), the spectral ratio curves would be straight lines.

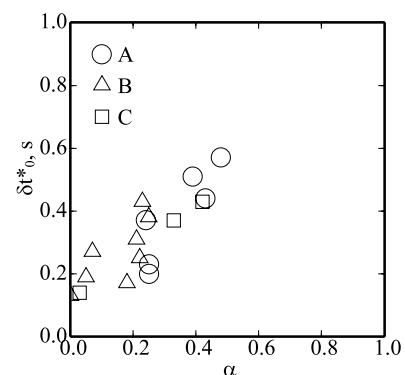


**Figure 5.** Optimum values of  $\alpha$  versus  $\delta t_0^*$  for each stack.

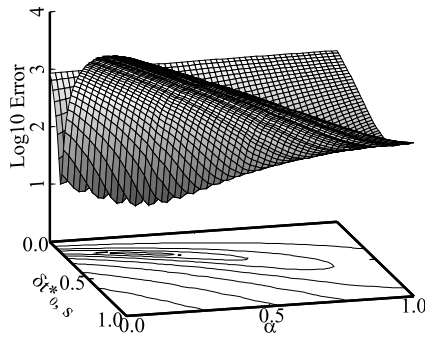


**Figure 6.** An example of RMS error surface for stacked spectral ratio curve (Figure 4b).

[15] Figure 5 shows the optimum values of  $\alpha$  and  $\delta t_0^*$  for each stack. Most spectral ratio stacks prefer  $0.2 < \alpha < 0.3$  for various  $\delta t_0^*$ . However, there is some scatter of  $\alpha$  ( $\alpha < 0.1$  or  $\alpha > 0.5$ ). The misfit surface derived from the grid search inversion (Figure 6) shows a positive tradeoff between estimated  $\alpha$  and  $\delta t_0^*$ , but allows wider variation in  $\delta t_0^*$  than in the exponent  $\alpha$ .

[16] We determined an aggregate value of  $\alpha$  by imposing the constraint that all spectral ratio stacks in a single event-group have the same  $\alpha$ , but different reference attenuations  $\delta t_0^*$ . The total misfit of all stacks in one group are used as a measure of fit. In the combined parameter fits, the optimum  $\alpha = 0.35$  for event-group A,  $\alpha = 0.14$  for event-group B, and  $\alpha = 0.29$  for event-group C. Therefore, spatial variation of attenuation in this region can be explained by an identical frequency dependence  $\alpha$  ( $0.1 < \alpha < 0.4$ ) with variations in reference attenuation  $\delta t_0^*$ .

## 5. Discussion

[17] We estimated the frequency dependence of seismic attenuation using  $P$ - $P$  spectral ratio method over the frequency range 0.08–8.0 Hz in the upper mantle beneath Japan. The observed frequency dependence can be expressed by a power-law  $Q(f) = Q_0(f/f_0)^\alpha$  with  $0.1 < \alpha < 0.4$ . We did not detect a change in the form of frequency dependence in this study (e.g., a composite power-law).

[18] Our estimates of the frequency dependence of seismic  $Q$  are consistent with laboratory experiments on solid olivine [e.g., Gueguen et al., 1989; Jackson et al., 2002]. This suggests that the physical process of attenuation in seismic wave propagation within Earth may be simulated adequately in laboratory experiments. Therefore, seismic wave attenuation measurements provide useful insights into physical (e.g., temperature) and/or chemical (e.g., water content) properties of Earth's interior when compared with experimental data on solid specimens.

[19] The observed frequency dependence of  $Q$   $0.2 < \alpha < 0.4$  in most regions is not consistent with the experimental results on partially molten olivine-rich rocks [Jackson et al., 2004; Faul et al., 2004]. Jackson et al. [2004] and Faul et al. [2004] showed that partial melting results in a broad peak in attenuation in the frequency range of  $10^{-2}$ –1 Hz causing weak frequency dependence in that frequency range. Such frequency dependence is not observed for most events in our study, suggesting that much of the observed attenuation is due to solid state processes. The deepest of

our three event-groups (event-group B), however, yields a frequency exponent  $\alpha = 0.14$ , far below laboratory-derived values on solid olivine suggesting the presence of partial melt in this region.

[20] Some studies of frequency dependent  $Q$  for much lower frequencies using Chandler wobble, tidal and free oscillation data [e.g., Anderson and Minster, 1979; Smith and Dahlen, 1981] indicate a frequency dependence of  $Q$  with  $\alpha = 0.1$ – $0.3$  for  $10^{-2}$ – $10^{-8}$  Hz. Combined with our results, this suggests a power-law behavior for a broad range of frequency ( $10^{-7}$ –10 Hz).

[21] **Acknowledgments.** The broadband seismogram records were provided by F-net (formerly FREESIA) operated by National Research Institute for Earth Science and Disaster Prevention seismograph networks in Japan and J-array operated by a consortium of universities. This research was partly supported by a Research Fellowship for Young Scientists from the Japan Society for the Promotion of Science and by NSF grant EAR-0208089.

## References

- Anderson, D. L., and J. B. Minster (1979), The frequency dependence of  $Q$  in the Earth and implication for mantle rheology and Chandler wobble, *Geophys. J. R. Astron. Soc.*, **58**, 431–440.
- Berckhemer, H., W. Kampfmann, E. Aulbach, and H. Schmeling (1982), Shear modulus and  $Q$  of forsterite and dunite near partial melting from forced-oscillation experiments, *Phys. Earth Planet. Inter.*, **29**, 30–41.
- Cheng, H.-X., and B. L. N. Kennett (2002), Frequency dependence of seismic wave attenuation in the upper mantle beneath the Australian region, *Geophys. J. Int.*, **150**, 45–57.
- Faul, U. H., J. D. Fitz Gerald, and I. Jackson (2004), Shear wave attenuation and dispersion in melt-bearing olivine polycrystals: 2. Microstructural interpretation and seismological implications, *J. Geophys. Res.*, **109**, doi:10.1029/2003JB002407, in press.
- Flanagan, M. P., and D. A. Wiens (1998), Attenuation of broadband  $P$  and  $S$  waves in Tonga: Observations of frequency dependent  $Q$ , *Pure Appl. Geophys.*, **153**, 345–375.
- Gueguen, Y., M. Darot, P. Mazot, and J. Woignard (1989),  $Q^{-1}$  of forsterite single crystals, *Phys. Earth Planet. Inter.*, **55**, 254–258.
- Jackson, I. (2000), Laboratory measurement of seismic wave dispersion and attenuation: Recent progress, in *Earth's Deep Interior: Mineral Physics and Tomography From the Atomic to the Global Scale*, *Geophys. Monogr. Ser.*, vol. 117, edited by S. Karato et al., pp. 265–289, AGU, Washington, D. C.
- Jackson, I., J. D. Fitz Gerald, U. H. Faul, and B. H. Tan (2002), Grain-size-sensitive seismic wave attenuation in polycrystalline olivine, *J. Geophys. Res.*, **107**(B12), 2360, doi:10.1029/2001JB001225.
- Jackson, I., U. H. Faul, J. D. Fitz Gerald, and B. H. Tan (2004), Shear-wave attenuation and dispersion in melt-bearing olivine polycrystals: 1. Specimen fabrication and mechanical testing, *J. Geophys. Res.*, **109**, doi:10.1029/2003JB002406, in press.
- Karato, S., and H. A. Spetzler (1990), Defect microdynamics in minerals and solid-state mechanisms of seismic wave attenuation and velocity dispersion in the mantle, *Rev. Geophys.*, **28**, 399–421.
- Romanowicz, B., and J. J. Durek (2000), Seismological constraints on attenuation in the Earth: A review, in *Earth's Deep Interior: Mineral Physics and Tomography From the Atomic to the Global Scale*, *Geophys. Monogr. Ser.*, vol. 117, edited by S. Karato et al., pp. 161–179, AGU, Washington, D. C.
- Roth, E. G., D. A. Wiens, L. M. Dorman, J. Hildebrand, and S. C. Webb (1999), Seismic attenuation tomography of the Tonga-Fiji region using phase pair methods, *J. Geophys. Res.*, **104**, 4795–4809.
- Shito, A., and T. Shibutani (2003), Anelastic structure of the upper mantle beneath the northern Philippine Sea, *Phys. Earth Planet. Inter.*, **140**, 319–329.
- Sipkin, S. A., and T. H. Jordan (1979), Frequency dependence of  $Q_{scs}$ , *Bull. Seismol. Soc. Am.*, **69**, 1055–1079.
- Smith, M. L., and F. A. Dahlen (1981), The period and  $Q$  of the Chandler wobble, *Geophys. J. R. Astron. Soc.*, **64**, 223–281.
- Ulug, A., and H. Berckhemer (1984), Frequency dependence of  $Q$  for seismic body waves in the Earth's mantle, *J. Geophys.*, **56**, 9–19.

A. Shito, S. Karato, and J. Park, Department of Geology and Geophysics, Yale University, 210 Whitney Avenue, New Haven, CT 06520, USA. (azusas@eri.u-tokyo.ac.jp)